DOI: https://doi.org/10.54966/jreen.v2i2.933 *Rev. Energ. Ren. Vol. 2 (1999) 99-108*

Microcrystalline Silicon Pin Solar Cells - Investigation of the Optoelectronic Properties -

Helmut Stiebig, Torsten Brammer, Juergen Zimmer,
Andreas Lambertz, Nadia Senoussaoui and Heribert Wagner

Forschungszentrum Jülich GmbH, ISI-PV, D-52425 Jülich, Germany
(Accepté le 29.11.99)

Abstract - *Microcrystalline silicon deposited by plasma enhanced chemical vapor deposition is a new material for solar cell applications. To optimize the cell performance microcrystalline solar cells deposited at different silane concentration (2 - 7.2 %) in hydrogen were investigated. For these cells four characteristic features were found: the dark current of the cells decreases, the open circuit voltage increases and the blue response is reduced with increasing silane concentration. The fill factor of the pin diodes shows a maximum of larger than 70 % for cells prepared at a silane concentration between 3.5 - 5.5 %. To study the transport and recombination of the diodes we have investigated the temperature dependence of these diodes and compared the experimentally determined optoelectronic properties with simulated data. The simulations reveal that the equilibrium carrier concentration of free carriers decreases and the influence of the nucleation region of the i-layer on the blue response increases with larger silane concentration.*

Résumé - *Du Silicium microcristallin déposé par la méthode de la déposition en phase vapeur augmentée par plasma est un nouveau matériau pour des applications solaires. Pour optimiser la performance de la cellule, des cellules microcristallines de différentes concentrations de silane (2 – 7.2%) en hydrogène ont été étudiées. Pour ces cellules, quatre propriétés caractéristiques ont été trouvées : le courant d'obscurité de la cellule décroît, la tension de court-circuit augmente et la réponse bleue diminue avec l'augmentation de la concentration en silane. Le facteur de remplissage des tiges de diodes présente un maximum supérieur à 70 % pour des cellules préparées à une concentration de silane entre 3,5 et 5,5 %. Pour étudier le transport et la recombinaison des diodes, nous avons examiné la dépendance de la température de ces diodes, et comparé les propriétés optoélectroniques déterminées expérimentalement avec les données simulées. La simulation révèle que la concentration à l'équilibre des porteurs libres décroît et l'influence de la région de germination de la couche i sur la réponse bleue augmente avec l'augmentation de la concentration de silane.*

Keywords: Microcrystalline silicon - Pin diodes - Solar cells - Nucleation region - thin-film technology.

1. INTRODUCTION

Microcrystalline silicon (μc-Si:H) promises the potential to combine the advantages of amorphous and crystalline silicon thin-film solar cells. Silicon is the second most abundant element in the Earth's crust and is non toxic. Deposition of microcrystalline silicon pin diodes is possible by thin-film technology, usually by plasma enhanced chemical vapor deposition (PECVD) [1], which distinguishes itself by easy control and small material consumption, and, using RF (radio frequency), as a commercial standard process. Low substrate temperatures (T = 150 – 250 °C) give the opportunity to use low-cost substrates such as standard glass or plastic foil [2]. The already developed monolithically integrated module technology redundantizes the current laborious solar cell interconnection for standard crystalline silicon wafer modules. The expectations for high efficiencies and stable performance are the driving force for the worldwide research activities on μc-Si:H. In comparison to amorphous silicon (a-Si:H) μc-Si:H shows no light induced degradation

behavior (Staebler-Wronski effect [3]) and an optical absorption similar to crystalline silicon (c-Si) [4]. High efficiencies for stacked a-Si:H/μc-Si:H pin structures [1] as well as for single μc-Si:H pin diodes [1, 5, 6] are achieved, but the transport and recombination behavior of μc-Si:H pin structures is not well understood and still under discussion.

Since device quality μc-Si:H grown by PECVD exhibits an anisotropic, columnar growth, the interpretation of the device behavior by the reflection of the material properties only is limited. The electronic properties of μc-Si:H are generally determined by conductivity and hall measurements, which yield information on the transport perpendicular to the growth direction due to the coplanar measurement set up. Further, the structural properties of our device quality μc-Si:H characterized by means of Raman spectroscopy, transmission electron microscopy (TEM) and X-ray diffraction (XRD) at grazing incidence show a crystallinity higher than 90 % and a crystallite size in the range between 5 and 40 nm [7]. Since small partially amorphous regions can not be detected by high resolution TEM due to lack of contrast, an experimental determination of the localization of the amorphous phase within the μc-Si:H material is very difficult [7]. This is complicated by the fact that it is not clear if the peak at 480 cm^{-1} in the Raman spectra, which is usually used to quantify the amorphous volume fraction, originates from an amorphous phase or from stressed bonds at grain boundaries [8]. Furthermore, in spite of extensive experimental work on the structure and properties of μc-Si:H a structural model for the grain boundaries consistent with the observations has not evolved and is discussed controversially.

To study the electronic transport and recombination behavior of μc-Si:H pin solar cells we developed a one and two dimensional (2D) numerical simulation program which takes into account the anisotropic structure. Thus, comparison of simulated and measured solar cell parameter gives deeper insight, because the transport of the carriers in growth direction of the columns are considered. This paper examines the optoelectronic properties of μc-Si:H pin solar cells with absorption layers deposited under different deposition conditions.

2. EXPERIMENT

The pin solar cells examined in this study were deposited in a multi-chamber glow discharge deposition system under very high frequency condition (VHF) of 95 MHz on glass substrates coated with non-textured transparent conductive oxide (TCO). Typical deposition conditions are a substrate temperature of 200 °C, deposition pressure of 300 mTorr and power of 5 W, yielding deposition rates between 1 and 3 Å/s.

The i-layers of the pin structures were deposited at different silane concentrations in hydrogen in the gas phase ($[SiH_4]/([SiH_4]+[H_2])$ varying from 2 % to 7.2 % with a thickness of 1 μm. The preparation conditions for the microcrystalline p- and the amorphous n-layers were kept constant. Measurements of the I/V-characteristics were carried out in the dark as well as under AM1.5 illumination in the temperature range between 250 - 350 K. The voltage and temperature dependent quantum efficiency (QE) was measured under a photon flux of less than 10^{14} $cm^{-2}s^{-1}$.

3. SIMULATION MODEL

The numerical simulation program is based on a modified version of our code which describes the optoelectronic behavior of a-Si:H pin structures and which includes a Fermi level dependent defect density in one and two dimensions [9]. The defect densities used are $5x10^{14}$ cm^{-3} and $5x10^{16}$ cm^{-3} in the crystallites and the grain boundaries, respectively. According to results of the bias light dependent QE the density of positively charged (D^p) and negatively charged (D^n) defects compared to the neutral ones (D^i) is reduced in comparison to a-Si:H.

In the crystallites we used electron and hole mobilities comparable to values in poly-Si and effective density of states at the band edges as found in c-Si. We assumed the µc-Si:H material to consist of crystalline grains (∅ ~ 15 nm) surrounded by thin (1 nm) grain boundaries with high defect density. Occurring band offsets are distributed in a ratio of 2:1 to the conduction band and valence band edge. The carrier generation in the structure is calculated taking into account coherent wave propagation within the coplanar multi-layer system [10]. For the µc-Si:H material we assumed the complex refractive indices of c-Si.

4. RESULTS AND DISCUSSION

4.1 Dark I/V curves of microcrystalline pin diodes

Since a comparison of the experimental and simulated dark I/V-curves allows insight into the transport and recombination behavior, we will first discuss the dark performance of µc-Si:H pin diodes with a silane concentration of 2 %. We started the simulations with the simplest assumption of an entirely crystalline i-layer. Figure 1 exhibits the differences between the measured (symbols) and the simulated (dots) data. In the low voltage region (V < 0.4 V) the dark current for the c-Si diode is up to two order of magnitude lower than the measured current of the µc-Si:H structure. At higher voltages the diodes show a high saturation current which is mainly limited by series resistances. This is in contrast to amorphous pin cells where the space charge limited current effect reduces the current density due to the high amount of charged defect states [11]. For the next approach we assumed that amorphous phase is located at the grain boundaries. The simulations show that the injection of electrons and holes at the contacts is strongly reduced leading to a decrease of the dark current by several orders of magnitude (dashed curve). This results in a sub-linear I/V-characteristics. In the last case grain boundaries with an increased defect density are introduced around the crystallites and crystalline properties for the crystallites are assumed. For this approach the dark current increases at low bias voltages (solid line) compared to the entirely c-Si i-layer and a good agreement with the experiment for the whole considered voltage range is achieved.

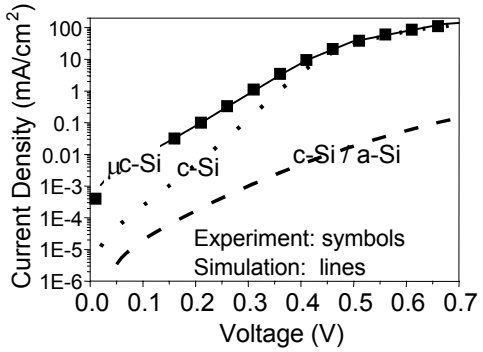

Fig. 1: Measured (symbols) dark I/V-curves of the µc-Si:H diode with a silane concentration of 2 % and simulated I/V-curves assuming an entirely c-Si i-layer (dots), defect rich grain boundaries around the crystallites (solid line) and barriers between the crystallites (dashed line).

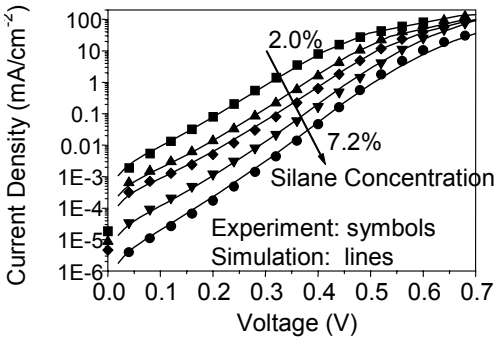

Fig. 2: Measured (symbols) and simulated (lines) dark I/V-curves as a function of the silane concentration (2.0 %, 3.5 %, 5.0 %, 6.5 %, 7.2 %).

Further, a comparison of experimental and simulated data has shown that amorphous phase distributed in the shape of larger regions has no significant effect on the solar cell

performance as long as the charge transport is dominated by 'crystalline' paths [9]. In areas where the charge carriers encounter a c-Si/a-Si barrier the electrons and holes are dammed up and evade the amorphous hindrance (amorphous phase distributed in the shape of larger regions) leading to high current densities perpendicular to the growth direction due to the free carrier gradients. Behind the hindrance the current flows together again. A prerequisite for an evading without a significant loss is a sufficient high conductivity of the crystalline regions to take over the additional current caused by the evading carriers [12]. Therefore, a random distribution of the amorphous phase in the shape of larger amorphous region is possible, since the influence on the transport is not significant and percolation is enabled. Beyond, a-Si:H could be located between the crystalline columns without major disturbance of the carrier transport.

However, the transport in microcrystalline silicon depends also on the deposition conditions of the absorption layer. One characteristic feature of the investigated silane series is a reduced dark current with increasingly high silane concentration. The measured and simulated dark I/V-curves of the silane series are shown in figure 2. With increasing silane content the curves are shifted parallely downwards to lower values. Numerical modeling reveals that this behavior is determined by the different bulk properties of the employed i-layer. This trend clearly indicates that the free carrier density (equilibrium concentration) within the i-layer decreases with increasing silane concentration. This can be described by a higher average mobility gap in the simulation. The average mobility gap was increased from 1.15 eV for the sample of 2 % to 1.35 eV for the sample of 6.5 %. The modeling results are in good agreement with the experimental data. The slight increase of the diode quality factor with decreasing silane flow can be attributed to an enhanced bulk recombination due to the higher equilibrium concentration in the bulk, analogous to the temperature dependent dark behavior of a-Si:H pin diodes. [11]

4.2 Solar cell parameters under AM1.5 illumination

The second characteristic feature of these samples is the open circuit voltage (V_{OC}) behavior which reflects the dark I/V characteristic of the cells (Fig. 2). With decreasing dark current, V_{OC} increases and a linear relation between V_{OC} and the silane concentration is observed between 2 % and 5 %. The slight sub-linear correlation for silane concentrations >5 % can be explained firstly by an increasing charge carrier recombination in the whole i-layer caused by a reduced extraction efficiency and secondly, by a steadily decreasing short circuit current (J_{SC}) which is 14.6 mA/cm^2 and 6.3 mA/cm^2 for the cell with 3.5 % and 7.2 %, respectively, whose origin will be discussed later. Since we have not taken into account possible changes in the dielectric constants of the material in the modeling, the drop in the short circuit current is in the simulations not as pronounced as in the experiment. Therefore, the slope of the V_{OC}-behavior is slightly higher than experimentally observed. The fill factor (FF) also shows a dependence on the silane concentration and exhibits a peak at a silane concentration of around 5 % (Fig. 3).

The increase in FF in the range between 2 - 5 % silane concentration can partly be attributed to an improved V_{OC} as known from ideal pn diodes [13]. The strong decrease of the FF for silane concentrations > 5 % gives a hint to limitations of the extraction properties in the bulk. The third characteristic feature is that the fill factor shows a maximum for solar cells with a medium silane concentration.

Figure 4 shows the temperature dependent FF behavior of the diodes. Due to the decreasing carrier mobility with higher temperature in the crystalline grains, the decrease of the FF is more pronounced for solar cells deposited with smaller silane concentration.

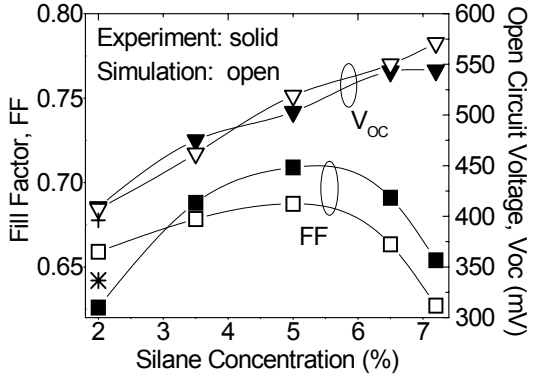

Fig. 3: Measured (filled symbols) and simulated (open symbols) V_{OC} and FF behavior as a function of the silane concentration. The cross and star denote the simulated values assuming a reduced conductivity in the p-layer.

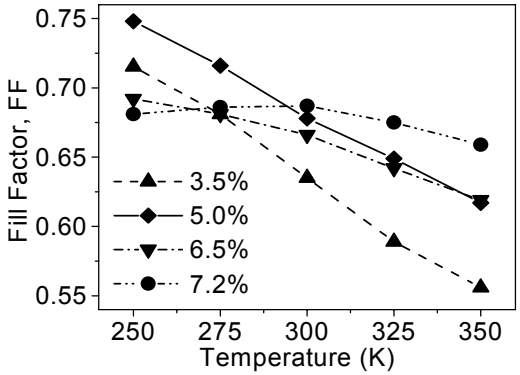

Fig. 4: Measured temperature dependent FF behavior as a function of the silane concentration.

With increasing silane concentration the influence of the grain boundaries on the carrier transport increases and the thermal activation of the carrier mobility there must be different in comparison to the grains. For the solar cell with a silane concentration of 7.2 % a nearly temperature independent FF is observed.

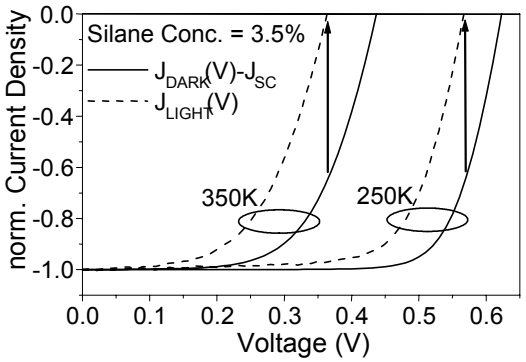

Fig. 5: Normalized measured and 'calculated' light I/V-curve for the solar cell with a silane concentration of 3.5 %.

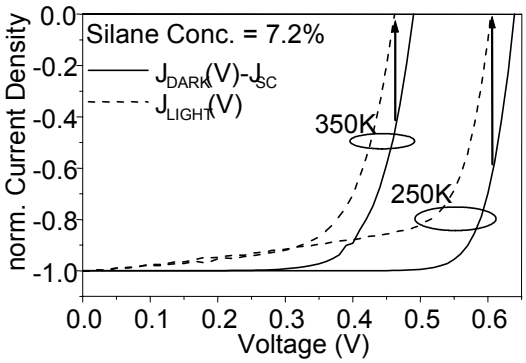

Fig. 6: Normalized measured and 'calculated' light I/V-curve for the solar cell with a silane concentration of 7.2 %.

This behavior is similar to solar cells based on a-Si:H [14]: the carrier mobility of a-Si:H shows no thermal activation in the investigated temperature range. These results demonstrate that this diode is prepared in the transition region between microcrystalline and amorphous growth.

The effect of temperature on the collection efficiency is displayed in more detail for the solar cells with a silane concentration of 3.5 % in figure 5 and of 7.2 % in figure 6. In each graph are plotted the measured light I/V-curve (solid line) and 'calculated light I/V-curve' (dashed line) which is based on the assumption of linear superposition of the dark current and photo-generated current ($J_{LIGHT}(V)=J_{DARK}(V)-J_{SC}$), [15]). The discrepancy between the measured and 'calculated' light I/V-curves for both silane concentrations reveals that the

simplifying assumption of a linear superposition of the dark and light current does not apply for these µc-Si:H pin diodes due to a considerable affect of the transit time on the light I/V-curve. Additionally, the splitting up between measured and 'calculated' (J_C) current varies with temperature depending on the silane concentration. The parameter describing this silane dependent behavior is the relative loss in current (J_C/J_{SC}) at the measured V_{OC}. For the 3.5 % sample, the relative loss is 0.7 at 250 K and 350 K. The two competing effects with increasing temperature, which are (1) the increasing potential across the absorber layer (due to the decreasing V_{OC}, not shown) and (2) the decreasing mobility, compensate each other for this silane concentration. However, for the 7.2 % sample the relative loss equals 0.7 at 250 K and 0.5 at 350 K. This indicates that the relative loss is dominated by the decreasing potential difference across the absorber layer. For a deeper insight into the spatially resolved transport and recombination behavior also the QE of the solar cells was investigated.

4.3 Quantum efficiency of microcrystalline pin diodes

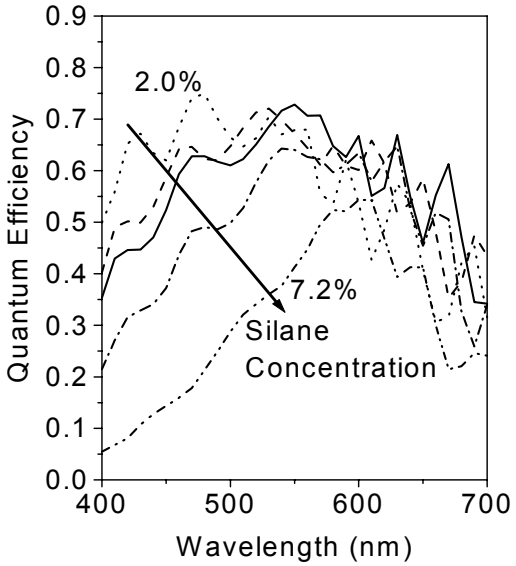

Fig. 7: Measured QE as a function of silane concentration (2.0 %, 3.5 %, 5.0 %, 6.5 %, 7.2 %) under short circuit condition.

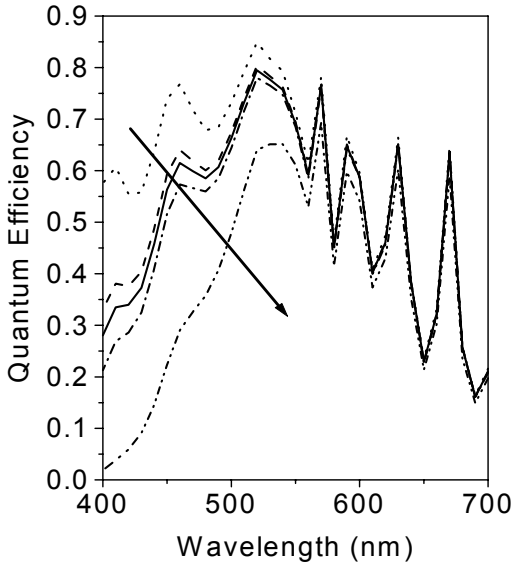

Fig. 8: Simulated QE as a function of silane concentration under short circuit condition.

Besides the I/V curves, also the external quantum efficiency measurements show a considerable dependence on the silane concentration. The main observation is the steadily decreasing spectral response for wavelengths from 300 to 550 nm as can be seen in figure 7 (fourth feature), measured under short circuit condition. Slight variations in the red response could originate from changes in the optical properties depending on the silane concentration. Modeling results are depicted in figure 8 and show again a very good agreement with the experimental findings. An increase of the average i-layer mobility gap in the simulations results in a band edge offset at the p/i-interface, so that the extraction of electrons photo-generated in the p-layer is increasingly hindered with a widening average i-layer mobility gap (i.e. silane concentration). Up to a silane concentration of ~ 5 % the drop of the QE in the blue/green wavelength region can be reproduced by the barrier at the p/i-interface alone. However, the deterioration of the blue response of the solar cell prepared with a silane flux exceeding 5 % can not be explained only by the impact of a barrier at the p/i interface on the carrier collection. The QE reveals an electron limiting transport process within the first 100 -

200 nm behind the p/i-interface showing evidence for an electronically active nucleation region in the μc-Si:H i-layer. This assumption is supported by detailed studies of the growth of single μc-Si:H films on c-Si as a function of the silane concentration in the gas phase [16]. Principally, this can be considered by including barriers between the crystalline grains or by reducing the free carrier mobility especially for the electrons in that region. We implemented additional barriers of 0 - 200 meV between the crystalline grains in the first 100 - 200 nm in dependence on the silane concentration.

This assumption is supported by the temperature dependence of the blue response as function of the silane concentration. The normalized temperature dependent QE at short circuit conditions for the 2 % and the 7.2 % sample is shown in Figure 9 and Figure 10, respectively. The QE at temperatures ranging from 250 K up to 350 K are normalized to the QE at 300 K. In the case that the QE(T) is higher than the measured curve at 300 K a value above 1 is calculated whereas a value below 1 indicates that the detected response is lower than the measured QE at room temperature. With increasing temperature the red response increases due to the decreasing optical bandgap. Thus, normalized QEs exceeding 1 are achieved for both structures. The appeared interference fringes can be attributed to the temperature dependence of the refractive indices and the thermal expansion of the device. The temperature dependent blue response of the devices differs significantly. In the 300 - 500 nm wavelength region a negative activation of the normalized QE is observed for the 2 % sample and a positive activation is measured for the 7.2 % sample. Furthermore, for samples with a silane concentration above 2 % the positive activation is more pronounced with increasing silane flow (not shown here). This positive activation can be explained as follows: at low temperatures the photo-generated carriers are hindered to overcome the barriers in the front part of the device. With increasing temperature and thermal activation the generated electrons surmount the obstacles. Thus, the blue/green response of the solar cells is influenced by the p/i-interface barrier in combination with a reduced extraction efficiency of carriers generated in the nucleation region. However, the 2 % sample, which exhibits neither a barrier at the p/i-interface nor a nucleation region, shows a negative activation of the blue response as a consequence of the decreasing carrier mobility with increasing temperature, as observed by the temperature dependence of the FF. (Fig. 4)

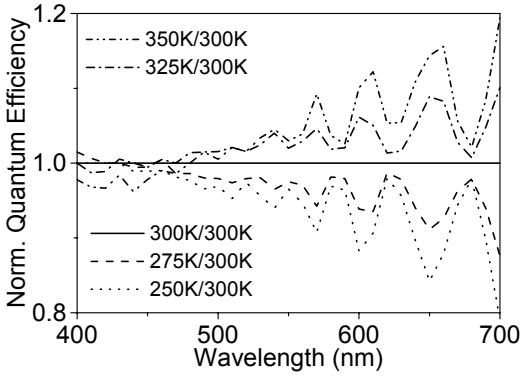

Fig. 9: Measured temperature dependent QE at short circuit conditions divided by the QE measured at 300 K for the 2 % structure.

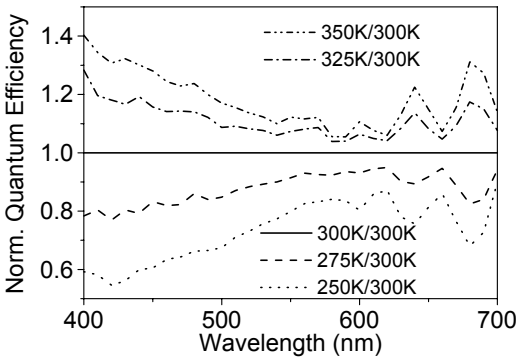

Fig. 10: Measured temperature dependent QE at short circuit conditions divided by the QE measured at 300 K for the 7.2 % structure.

Further information can be deduced by the investigation of the voltage dependent QE. As an example the normalized QE of the sample with 3.5 % and 7.2 % silane concentration are plotted in figure 11. The diagram exhibits the curves of the measured and the simulated

quantum efficiency at 0.4 V forward bias normalized to the short circuit case in order to monitor the spatially dependent changes of the extraction properties when the internal field strength is weakened. Both curves show an increasing reduction of the blue sensitivity in comparison to the red sensitivity whereas the bias dependent drop of the blue response is more pronounced with rising silane concentration. This behavior is mainly determined by the influence of the nucleation region and the p/i-interface on the carrier extraction. Regarding the whole spectrum, the lower absolute values of the QE of the 7.2 % solar cell in comparison to the sample deposited with lower silane flow (3.5 %) can be attributed to a reduced carrier collection efficiency in the total i-layer. This behavior can be described in the simulations by the inclusion of small barriers (0-50 meV) between the crystalline grains in the whole i-layer in addition to the 'nucleation region', thereby affecting the transport behavior of the carriers in the bulk of the absorption layer for the samples with a silane flow above 5 %. This is in accordance with the assumption made for "high silane" material based on the dark and illuminated I/V characteristics. Since the 2 % sample shows a nearly wavelength independent decrease of the QE with increasing forward bias (Fig. 12), no indication was found for a significant nucleation region with affect on the transport properties in the front part for material prepared with low silane concentration. Thus, the study demonstrates that both, the properties of the nucleation region and the quality of the bulk material depend on the deposition conditions and can be varied from fully crystalline to more "amorphous-like".

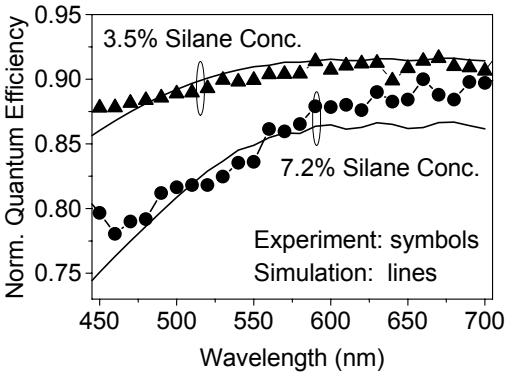

Fig. 11: Simulated (lines) and measured (symbols) QE at 0.4 V forward bias normalized to the short circuit case.

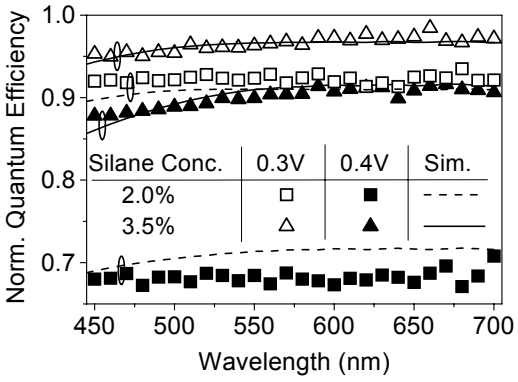

Fig. 12: Simulated (lines) and measured (symbols) QE at 0.3 V and 0.4 V forward bias normalized to the short circuit case.

Up to now, the simulations of the investigated structure are carried out with the same set of parameters differing only in the bandgap structure of the i-layer. However, the voltage dependence of the 2 % solar cell can be better reproduced in the simulation by a reduction of the conductivity in the p-layer. Figure 12 shows the normalized QE measured of the samples prepared with 2 % and 3.5 % silane concentration. The QE curves are measured at 0.3 V and 0.4 V are divided by the QE detected under short circuit conditions. In contrast to the discussion above the normalized QE of the 2 % sample is lower than the normalized QE of the 3.5 % sample. At 0.4 V forward bias, the red response for solar cells prepared with a silane concentration larger than 2 % was above 85 % (Fig. 11). Only the 2 % solar cell showed a more pronounced voltage dependence (Fig. 12). Therefore, in the simulation the Fermi level is shifted from 0.2 eV to 0.3 eV to reduce the built-in potential. Taking into account this modification for the 2 % sample also the agreement between the simulated and measured V_{OC} and FF (cross and star in figure 3) can be improved. Due to the reduced built-

in potential, V_{OC} and the FF decreases. The deposition of the i-layer at low silane concentrations (i.e. high hydrogen concentration) could lead to a hydrogenation of the μc-Si:H p-layer, thereby resulting in a partly electronic deactivation of the boron atoms [17], giving rise to a lower activation energy in the p-layer and a smaller built-in electric field in the i-layer. These results demonstrate that the transport in microcrystalline diodes is multifaceted and depends strongly on the deposition conditions. Due to the dependence of the FF and V_{OC} on the silane concentration, the highest efficiency is obtained in the deposition regime at a silane concentration around 5 %.

Similar trends are observed for solar cells deposited on textured TCO. Due to the better utilization of the solar cell spectrum caused by an improved light trapping especially in the long wavelength range [6, 18] the short circuit current for this series prepared on textured TCO front contact lies between 15-21 mA/cm^2 depending on the silane concentration.

5. CONCLUSION

The solar cell performance depends strongly on the deposition conditions. A comparison of experimental results and numerical simulations shows that the observed silane concentration dependence regarding the dark I/V-behavior and V_{OC} can be explained in terms of a reduced equilibrium carrier concentration. The decreasing blue response with higher silane dilution can be attributed to a conduction band offset at the p/i-interface and additional barriers in the nucleation region of the i-layer. The assumption of barriers is supported by temperature dependent QE measurements which show a positive activation for increased temperatures. Although the i-layer quality rises with lower silane concentration, a high efficiency can be observed for μc-Si:H solar cells deposited at a silane concentration between 3.5 % and 5.5 % due to the silane concentration dependence of the FF and V_{OC}.

Acknowledgement : The authors thank F. Finger, W. Reetz and O. Vetterl for helpful discussions. This work was supported by the Bundesministerium für Bildung und Forschung (BMBF). N. Senoussaoui thanks Deutscher Akademischer Austauschdienst (DAAD) for funding of her stay at Forschungszentrum Jülich.

REFERENCES

[1] J. Meier, P. Torres, R. Platz, S. Dubail, U. Kroll, J.A. Anna Selvan, N. Pellaton Vaucher, Ch. Hof, D. Fischer, H. Keppner, A. Shah, K-D. Ufert, P. Giannoules and J. Koehler, Mater. Res. Soc., Proc, 420, (1996), 3.

[2] J. Kanicki, Ed. '*Amorphous and microcrystalline Semiconductor Devices*', Boston: Artech House, (1991).

[3] D.L. Staebler and C.R. Wronski, J. Appl. Phys. 51, (1977), 292

[4] R. Carius, F. Finger, U. Backhausen, M. Luysberg, P. Hapke, L. Houben, M. Otte and H. Overhoff, Mater. Res. Soc., Proc, 467, (1997), 283.

[5] K. Yamamoto, M. Yoshimi, T. Suzuki, Y. Tawada, Y. Okamoto and A. Nakajima, Proc. 2nd World Conference and Exhibition on Photovoltaic Solar Energy Conversion, Vienna, Austria (1998).

[6] O. Vetterl, P. Hapke, O. Kluth, A. Lambertz, S. Wieder, B. Rech, F. Finger and H. Wagner, Solid State Phenomena, 67-68, (1999), 101.

[7] M. Luysberg, P. Hapke, R. Carius and F. Finger, Phil. Mag. A75, (1997), 31.

[8] S. Veprek, F.-A. Sarott and Z. Iqbal, Phys. Rev. B, 36, (1987), 3344.

[9] J. Zimmer, H. Stiebig and H. Wagner, Mater. Res. Soc., Proc, 507, (1998), 377.

[10] H. Stiebig, A. Kreisel, K. Winz, M. Meer, N. Schultz, C. Beneking, Th. Eickhoff and H. Wagner, Proc. First World Conference on Photovoltaic Energy Conversion (WCPEC), (1994), 603.
[11] Th. Eickhoff, H. Stiebig, W. Reetz, B. Rech and H. Wagner, Proc. 13th European Photovoltaic Solar Energy Conference, Nice, (1995), 238.
[12] J. Zimmer, H. Stiebig, P. Hapke and H. Wagner, Proc. 2nd World Conference and Exhibition on Photovoltaic Solar Energy Conversion (WCEPSEC), Vienna, Austria, (1998), 944.
[13] M. A. Green, in '*Solar Cells*', Prentice-Hall Inc., Englewood Cliffs, N.J., (1982).
[14] H. Stiebig, Th. Eickhoff, J. Zimmer, C. Beneking and H. Wagner, Mater. Res. Soc., Proc. 420, (1996), 855.
[15] S. M. Sze, '*Physics of Semiconductor Devices*', John Wiley & Sons, (1981).
[16] L. Houben, M. Luysberg, P. Hapke, R. Carius, F. Finger and H. Wagner, Phil. Mag. A, 77, (1998), 1447.
[17] J.I. Pankove, D.E. Carlson, J.E. Berkeyheiser and R.O. Wance, Phys. Rev. Lett., 51, (1983), 2224.
[18] N. Senoussaoui, T. Repmann, T. Brammer, H. Stiebig and H. Wagner, Journées Nationale de Valorisation des Energies Renouvelables, Tlemcen, Algeria, (1999).